
Original Article

Cell growth of the mouse SDHC mutant cells was suppressed by apoptosis throughout mitochondrial pathway

Masaki Miyazawa^{1,*}, Takamasa Ishii^{1,*}, Mika Kirinashizawa¹, Kayo Yasuda¹, Okio Hino², Philip S. Hartman³, Naoaki Ishii^{1,**}

¹ Department of Molecular Life Science, Division of Basic Medical Science and Molecular Medicine, Tokai University School of Medicine, Isehara, Kanagawa, Japan;

² Department of Pathology (II), Juntendo University School of Medicine, Bunkyo-ku, Tokyo, Japan;

³ Department of Biology, Texas Christian University, Fort Worth, Texas, USA.

Summary

SDHC E69 cells, which overproduce superoxide anions in their mitochondria, were previously established that had a mutation in the SDHC gene of complex II of the respiratory chain. We now demonstrate that tumors formed by NIH 3T3 and SDHC E69 cells showed significant histological differences. Cytoplasmic cytochrome c release from mitochondria was significantly elevated in SDHC E69 cells and was likely caused by superoxide anion overproduction from mitochondria. In addition, the p53 and Ras signal transduction pathways were activated by oxidative stress and may play a key role in the supernumerary apoptosis in SDHC E69 cells. Our results suggest that the development and growth characteristics of hereditary paragangliomas, which are defective in the same complex of electron transport as mouse SDHC E69 cells, may be caused by apoptosis induction by mitochondrial oxidative stress.

Keywords: Mitochondria, Superoxide anion, Oxidative stress, Apoptosis, Paraganglioma

1. Introduction

Major endogenous reactive oxygen species (ROS) are generated from electron leakage during cellular respiration in mitochondria (1). The *mev-1* mutant of the nematode *Caenorhabditis elegans* is mutated in the SDHC subunit of complex II in electron transport system (2) and produces excessive superoxide anions (O_2^-) in its mitochondria (3). This mutant has proven extremely useful for the study of endogenous oxidative stress and its effects on lifespan, apoptosis and mutagenesis (4,5). We have recently constructed a transgenic mouse cell line (SDHC E69 cells) with a mutation that mimics *mev-1* (6). As in *C. elegans*, excess O_2^- were generated, which led to supernumerary apoptosis and hypermutability (6). Interestingly, the

SDHC E69 cells that escaped from apoptosis were frequently transformed and, when the cells were injected under the epithelium of nude mice, they resulted in the production of tumors two weeks after implantation (6). Conversely, after wild-type cells (NIH3T3 cells) were injected, they were on the verge of disappearance but were transformed at high frequency by spontaneous mutations during long passage time or culture time. We show in this report that the NIH3T3 wild-type tumors developed with considerable proliferative abilities over the course of further incubation while the tumor mass of SDHC E69 transformed cells did not significantly enlarge.

It has been reported that mutations in the SDHC or SDHD gene of mitochondrial complex II cause some nonchromaffin and hereditary paragangliomas (PGLs) in humans (7,8). Therefore, further analysis of SDHC E69 cells may help clarify the molecular mechanism of the tumorigenesis in neoplasms such as PGLs. It is clear that apoptosis and cell-cycle arrest serve as defensive mechanisms to rid organisms from potentially neoplastic cells. However, the molecular mechanisms by which apoptosis is stimulated by ROS overproduction

*These authors contributed equally to this work.

**Correspondence to: Dr. Naoaki Ishii, Department of Molecular Life Science, Division of Basic Medical Science and Molecular Medicine, Tokai University School of Medicine, 143 Shimokasuya, Isehara, Kanagawa 259-1193, Japan; e-mail: nishii@is.icc.u-tokai.ac.jp

from mitochondria are not completely understood. In this report, we explored the mitochondrial and cytosolic responses on apoptosis to ROS overproduction in SDHC E69 mitochondria. Specifically, excess apoptosis in SDHC E69 cells was mediated virtually exclusively through the mitochondrial pathway. In addition, p53 and Ras-MEKK pathways were presumably stimulated in the SDHC E69 cells.

2. Materials and Methods

2.1. Cell culture

The cells were cultivated in DMEM medium (Nissui Company, Tokyo) including 2.5% FBS + 2.5% CS in a 5% CO₂ incubator. Cell division and proliferation were examined after synchronous culture in G0 phase into exhaustion of serum medium and at the contact inhibition state in 100-mm tissue culture dishes. For cell growth, 5×10^4 synchronized cells were cultured in a standard medium of 35-mm tissue culture dishes.

In this manuscript, three-month SDHC E69 cells after the establishment and their wild-type cells (NIH3T3 cells) for 3 month cultured cells as progenitors were used. In brief, the three-month SDHC E69 cells showed the loss of contact inhibition and had many apoptotic molecule-like granules during the first month after establishment (6). During the period of colony formation, some clefts characteristics of programmed cell death were found in the center of some colonies (6). In the SDHC E69 cells, the morphology was changed from the typical solid and elongated fibroblasts to smooth and rounded cells (6). Similar changes were evident, although to a lesser degree in the one-month SDHC E69 cells after establishment (6). In addition, the three-month SDHC E69 cells formed multiple layers (6).

2.2. Antibodies and chemicals

Caspase inhibitors Z-Leu-Glu(OMe)-Thr-Asp-(OMe)-FMK (an inhibitor of caspase 8) and Z-Leu-Glu(OMe)-His-Asp(OMe)-FMK (an inhibitor of caspase 9) were purchased from ICN Pharmaceuticals (Irvine). p53 antibody, phospho-p53 (Ser15) antibody, phospho-p38 MAP kinase (Thr180/Tyr182) antibody, phospho-SAPK/JNK (Thr183/Tyr185) antibody and Bid antibody were purchased from Cell Signaling Technology. p21 (C-19) antibody, Bax (N-20) antibody and MEK kinase-1 (C-22) were purchased from Santa Cruz Biotechnology, Inc (Santa Cruz). Anti-cytochrome c monoclonal antibody was purchased from BD PharMingen (San Jose). Anti-rabbit Ig, horseradish peroxidase linked F(ab')₂ fragment (from donkey) and anti-mouse Ig, horseradish peroxidase linked F(ab')₂ fragment (from sheep) were purchased from Amersham Pharmacia Biotech. The luciferase reporter gene pp53-TA-Luc and pTA-Luc vector used in the p53 reporter assay were

purchased from Clontech.

2.3. Transfection and luciferase assay

An AP-1 cis-element dependent transcriptional expression vector (pAP-1-TA-Luc) was constructed using the AP-1 cis-element 5' primer (CTAGCTGAGT CAGTGAGTCACTGACTCACTGACTCATGAGTCA GCTGACTCA) and the AP-1 cis-element 3' primer (G ATCTGAGTCAGCTGACTCATGAGTCAGTGAGTC AGTGACTCACTGACTCAG). These were annealed, and this oligonucleotide was inserted at an *NheI*-*Bgl*III site in the pE2F-TA-Luc plasmid vector without the E2F binding site. A pE2F-TA-Luc plasmid vector without the E2F binding site (p-TA-Luc) was used as the negative control vector. Transient transfection of pp53-TA-Luc (0.5 µg), pTA-Luc (0.5 µg) and pCMV-β-galactosidase (0.05 µg) or pAP-1-TA-Luc (0.5 µg), p-TA-Luc (0.5 µg) and pCMV-β-galactosidase (0.05 µg) into NIH3T3 and SDHC E69 cell lines was performed using LipofectAMINE Plus reagent (Invitrogen Inc.). Proteins were prepared for luciferase and β-galactosidase analysis 48 h after transfection by addition of lysis buffer (0.625 mM Tris-PO₄ (pH 7.8), 15% glycerol, 2% CHAPS, 1% Lecichin (*L*-α-phosphachigilcholine), 1% BSA, 0.1 M EGTA, 1 M MgCl₂, 1 M DTT, 0.1 M *p*-APMSF). These protein lysates were measured for luciferase and β-galactosidase activities using Luminescencer-PSN (ATTO) or SPECTRA MAX 250 (Molecular Devices) after addition of luciferase buffer (20 mM Tricine-NaOH, 1 mM 4MgCO₃ • Mg(OH) • 5H₂O (pH 2.3), 2.7 mM MgSO₄ • 7(H₂O) (pH 2.3), 0.1 mM EDTA, 33 mM DTT, 0.27 mM CoA-Li, 0.47 mM luciferin, 0.53 mM ATP) or β-galactosidase buffer (60 mM Na₂HPO₄ • 12H₂O, 10 mM KCl, 1 mM MgCl₂, 40 mM NaH₂PO₄ • 2H₂O, 1.1 mM ONPG, 47.5 mM 2-mercaptoethanol). Samples were then incubated for 1 h at 37°C. Luciferase relative activity was normalized based on β-galactosidase activity levels and luciferase activity levels of p-TA-Luc, pTA-Luc negative control vector.

2.4. Northern blot analysis

Mouse cDNA's for Northern blot analysis were obtained by RT-PCR method using oligonucleotides for MDM2 (5'-GCC ACC AGA AGA GAA ACC-3' and 5'-GCC TGA GCT GAG TTT TCC-3'), p21-Ras (5'-TTG GAG CAG GTG GTG TTG-3' and 5'-ACA CAT CAG CAC ACA GGG-3'), M-Ras (5'-AGT AGT GGT GGG AGA TGG-3' and 5'-AGT TTG TGA GTG CCG GTG-3'), Raf-1/C-Raf (5'-CAT GAG CAC TGT AGC ACC-3' and 5'-ATC TCC ATG CCA CTT GCC-3'), 18s rRNA (5'-TAC CTG GTT GAT CCT GCC-3' and 5'-TTT CGT CAC TAC CTC CCC-3'), actin (5'-TGG AGA AGA TCT GGC ACC-3' and 5'-ACC CAA GAA GGA AGG CTG-3'), and G3PDH (5'-CAC GGC AAA TTC AAC

GGC-3' and 5'-CTT GGC AGG TTT CTC CAG-3'). 3 µg of mRNA which was extracted by Oligotex-dT30 Super (Roche) was subjected to Northern Blot analysis. Mouse cDNA's were random-prime-labeled using the High prime kit (Roche) with ³²P-dCTP (Amersham Biosciences) and purified using ProbeQuant G-50 Micro Columns (Amersham Biosciences). After hybridization for mouse cDNA's filters were stripped and reprobed for actin and G3PDH to verify that comparable amounts of RNA had been loaded in all lanes.

2.5. Western blot analysis

After a particular treatment, cells were washed twice with phosphate buffered saline and incubated on ice in lysis buffer containing 10 mM Tris-HCl (pH 8.0), 1 mM EDTA, 100 mM NaCl, 0.1% NP-40, 1 mM DTT and 0.1 mM *p*-APMSF for 10 min. This was followed by brief sonication for Western blot analysis of p53 or p21. Cell lysates for p21 analysis were then cleared by centrifugation (400 × *g*) for 5 min, and the supernatants were used. In Western blot analysis of Bax or cytochrome *c*, both the mitochondrial and cytoplasm fractions were employed. These cell lysates (containing 10-100 µg of protein) were solubilized by boiling after the addition of 2 × SDS-PAGE sample buffer (0.125 M Tris-HCl (pH 6.8), 10% 2-mercaptoethanol, 4% SDS, 10% sucrose and 0.004% bromophenol blue). For the analysis of p38, p-JNK, Bid or MEKK1, cells were washed twice with phosphate buffered saline and incubated in SDS-PAGE sample buffer containing 62.5 mM Tris-HCl (pH 6.8), 2% SDS, 50 mM DTT and 10% glycerol for 10 min on ice followed by brief sonication. Cell lysates were then cleared by centrifugation (400 × *g*) for 5 min and the supernatants were directly subjected to SDS-PAGE. After electrophoresis, the proteins were transferred to PVDF (polyvinylidene difluoride) membrane Clearblot membrane (ATTO) using a Semi-dry blotting machine AE-6677 (ATTO). To block nonspecific protein binding, membranes treated for 8 h at 20-25°C with either 0.1% Tween 20, 5% nonfat dried milk in phosphate buffered saline for analyses of p53, p21, Bax, cytochrome *c*, Bid or MEKK1 or 5% bovine serum albumin, 0.1% Tween 20 in TBS (0.02 M Trizma base, 0.137 M NaCl (pH 7.6)) for analyses of phospho-p53 (Ser15), phospho-p38 MAP kinase (Thr180/Tyr182) or phospho-SAPK/JNK (Thr183/Tyr185). The membranes were treated with anti- p53, p21, Bax, cytochrome *c*, or MEKK1 antibody in phosphate buffered saline containing 0.1% Tween 20, 5% nonfat dried milk, or phospho-p53 (Ser15) antibody in TBS containing 0.1% Tween 20, 5% bovine serum albumin at room temperature for 1 h or with Bid antibody in phosphate-buffered saline containing 0.1% Tween20, 5% nonfat dried milk, or phospho-p38 MAP kinase (Thr180/Tyr182) or phospho-SAPK/JNK (Thr183/Tyr185) antibody in TBS containing 0.1%

Tween 20, 5% bovine serum albumin at 4°C for 8 h. The membranes were then washed with the antibody dilution buffer for 30 min. They were then treated with the ECL-plus Western blotting detection system (Amersham Biosciences) after treatment with anti-rabbit or anti-mouse antibody (for analysis using Bid). They were then exposed to Hyperfilm™ ECL chemiluminescence film (Amersham Biosciences) at room temperature for 2 min. The chemiluminescent signals were visualized with a CS Analyzer and AE-6962 light capture (ATTO).

3. Results

3.1. Morphology of the SDHC E69 cells on nude mouse

It is known that NIH3T3 cells are transformed at high frequency by spontaneous mutations during long passage time or culture time. In fact, the cells, which did not proliferate within two weeks after the injection under the epithelium of nude mice (Figure 1A), grew into huge malignant tumors one month (Figure 1B). Some of the SDHC E69 cells that escaped from apoptosis underwent transformation, as evidenced by the fact that SDHC E69 transformed cells caused tumors within two weeks when injected under the epithelium of nude mice (Figure 1C) (6). The size of tumors remained unchanged even after one and a half month (Figure 1D). As expected of actively proliferating neoplasms, the tumors derived from the NIH3T3 cells had evidence of the apocytes and the nuclear divisions with characteristic dense staining of the cytoplasm (Figure 2A). In addition, the margin between the tumor and the blood vessel was distinct (Figure 2B). In contrast, The SDHC E69-derived tumors showed no evidence of nuclear divisions and showed nuclear aggregation (Figure 2C). They had assumed the posture of a fibrous tumor, and the blood vessel and tumor border was not distinct. Moreover, tumor-associated cells were present (Figure 2D). Thus, the thickness of the tumor cells layer was less when derived from SDHC E69 cells (Figure 2F) versus the wild type cells (Figure 2E).

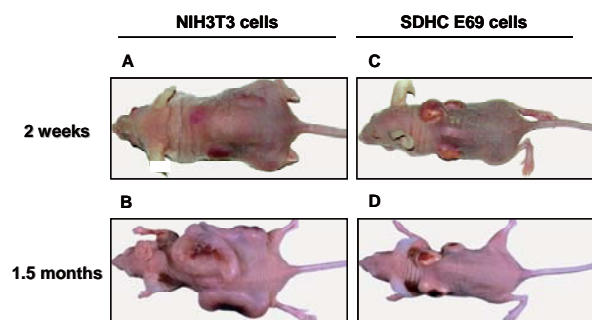


Figure 1. Comparisons of tumorigenesis using NIH3T3 cells and SDHC E69 cells injected into the epithelia of nude mice and cultured for two weeks and one and a half-months. Transplantation of spontaneous transformation NIH3T3 cells (A and B) and SDHC E69 cells (C and D) in epithelia of nude mice.

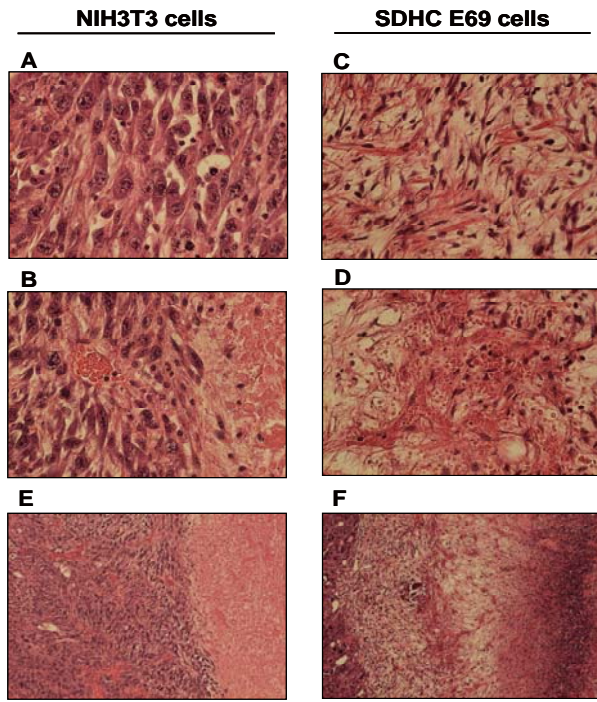


Figure 2. The tissue specimen of the tumor into epithelia of nude mice in spontaneous transformation NIH3T3 cells (A, B, E) and in SDHC E69 cells (C, D, F).

3.2. The role of mitochondrial function to apoptosis

Cellular cytochrome c was found in the mitochondria in both the SDHC E69 cells and NIH3T3 cells (Figure 3A). Cytosolic levels in the SDHC E69 cells and NIH3T3 cells were lower than mitochondrial levels. However, cytosolic cytochrome c levels increased significantly in the SDHC E69 cells.

In the mitochondria of the SDHC E69 cells compared to NIH3T3 cells, the Bax levels were significantly higher (Figure 3A). Bid and tBid levels were barely detectable in the SDHC E69 cells (Figure 3A).

In NIH3T3 cells, MDM2 mRNA expression was equally distributed between the 3.0 kbp and 1.7 kbp mRNAs, which are translated into the p90 and p76 MDM2 proteins, respectively (Figure 3B). A dramatically different pattern was observed in the SDHC E69 cells, as only the short-form type was expressed, which is incapable binding to and promoting p53 protein degradation (Figure 3B). p53 protein levels were below the level of detection in NIH3T3 cells (Figure 3C). Conversely, p53 protein existed in copious

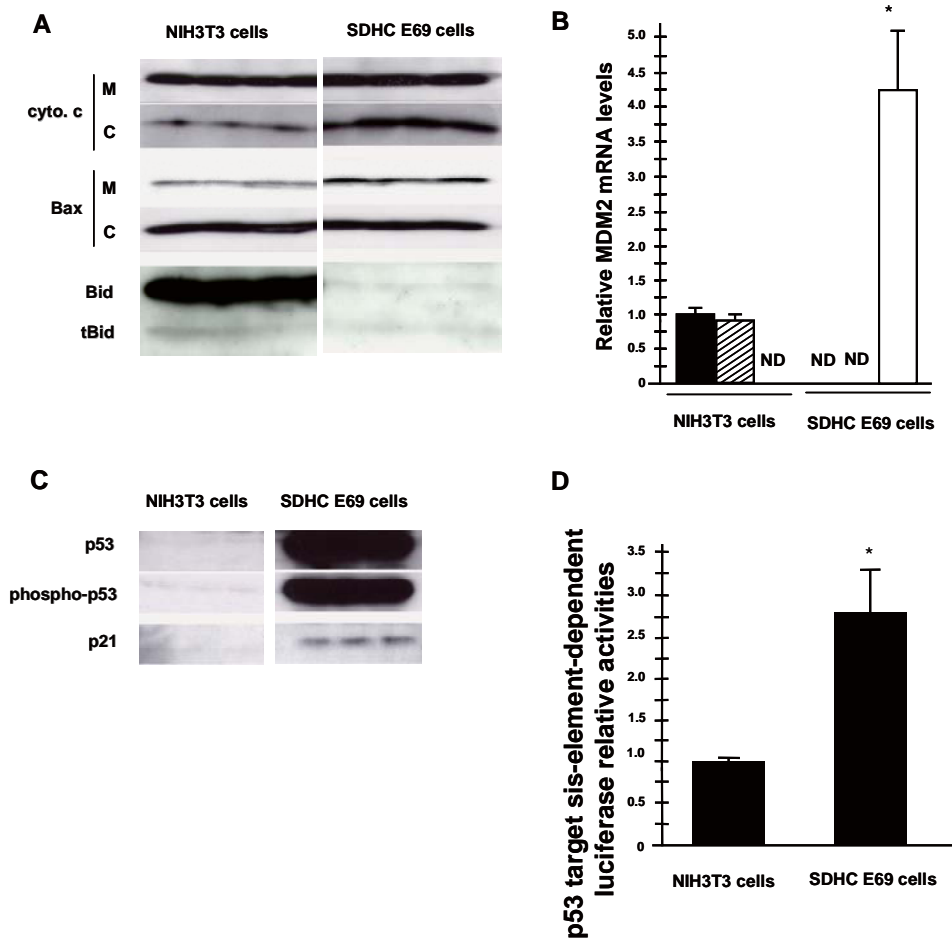


Figure 3. The alteration of cytochrome c release, inducible protein localization and p53 activation in NIH3T3 and SDHC E69 cells. A: Detection of cytochrome c, Bax and Bid proteins levels by Western blot analysis. cyto. c: cytochrome c, M: mitochondrial fraction, C: cytoplasmic fraction. *n* = 3. B: Detection of MDM2 mRNA patterns and expression levels by Northern blot analysis. MDM2 mRNA patterns of 3.0 kbp (p90, full-length MDM2) (closed boxes), 1.7 kbp (p76, not containing p53 binding motif) (hatched boxes) and 1.0 kbp (short form, not containing proteins binding motif) (open boxes) were detected. * *p* < 0.01, *n* = 3. C: Detection of p53, phospho-p53 and p21 protein levels by Western blot analysis. *n* = 3. D: Measurement of p53-dependent transcriptional activation levels by p53 target cis-element-dependent luciferase activity. * *p* < 0.01, *n* = 3.

amounts in the SDHC E69 cells, in which the short-form type MDM2 mRNA was expressed (Figure 3C). Moreover, most of the p53 protein was phosphorylated at serine residue 15 (Figure 3C). In addition, p21 protein was highly expressed in the SDHC E69 cells but not in NIH3T3 cells (Figure 3C). In the each cell lines transiently transfected a luciferase-containing construct with a p53 binding cis-elements, luciferase activity was over 2.8 times higher in the SDHC E69 cells than in the NIH3T3 cells (Figure 3D).

3.3. The role of caspase 8 and caspase 9 on apoptosis

As demonstrated previously, caspase 3 levels were higher in the SDHC E69 cells than in NIH3T3 cells (Figure 4A) (6). In the NIH3T3 cells, caspase 3 activity was slightly decreased by each caspase antagonist ($p < 0.01$) (Figure 4A). Caspase 3 activity was not further reduced by addition of both caspase 8 and 9 antagonists in the NIH3T3 cells (Figure 4A). In the SDHC E69 cells, both caspase 8 and caspase 9 inhibition had a larger effect on caspase 3 activity (Figure 4A). Moreover, we tested the viability of cells cultured in the presence of each caspase antagonist. The survival rate of the NIH3T3 cells was decreased by treatment with a caspase 9 antagonist (Figure 4B).

In contrast to the results obtained with NIH3T3 cells, the presence of each caspase antagonist resulted in increased the cell growth and proliferation in the SDHC E69 cells (Figure 4C). Moreover, both caspase 8 and 9 antagonists were inadequate to substantially reduce caspase 3 activity in the SDHC E69 cells ($p < 0.01$) (Figure 4A).

3.4. The role of transduction pathway to apoptosis and tumorigenesis

First, we analyzed p21Ras (H-, N-, K-Ras) and M-Ras mRNA expression levels by Northern blot analysis. Relative to the actin and G3PDH internal controls, p21Ras and M-Ras mRNA expression levels in the SDHC E69 cells were increased in comparison with the NIH3T3 cells (Figure 5A).

Relative to the actin and G3PDH internal standards, Raf-1/C-Raf mRNA expression, which induces cell growth and proliferation, was significantly increased in the SDHC cells in comparison to the NIH3T3 cells (Figure 5B). 195 kDa full-length MEKK1 protein was present in unchanged amount in the SDHC E69 cells, but the activated p91kDa MEKK1 protein was increased (Figure 5C). In addition, activated 54 kDa and 46 kDa JNK proteins were present in increased amounts in the SDHC E69 cells (Figure 5C). Conversely, the accumulation of activated p38 MAPK protein was not altered (Figure 5C). An AP-1 cis-element-dependent luciferase assay showed that JNK-dependent transcription was activated in the SDHC E69

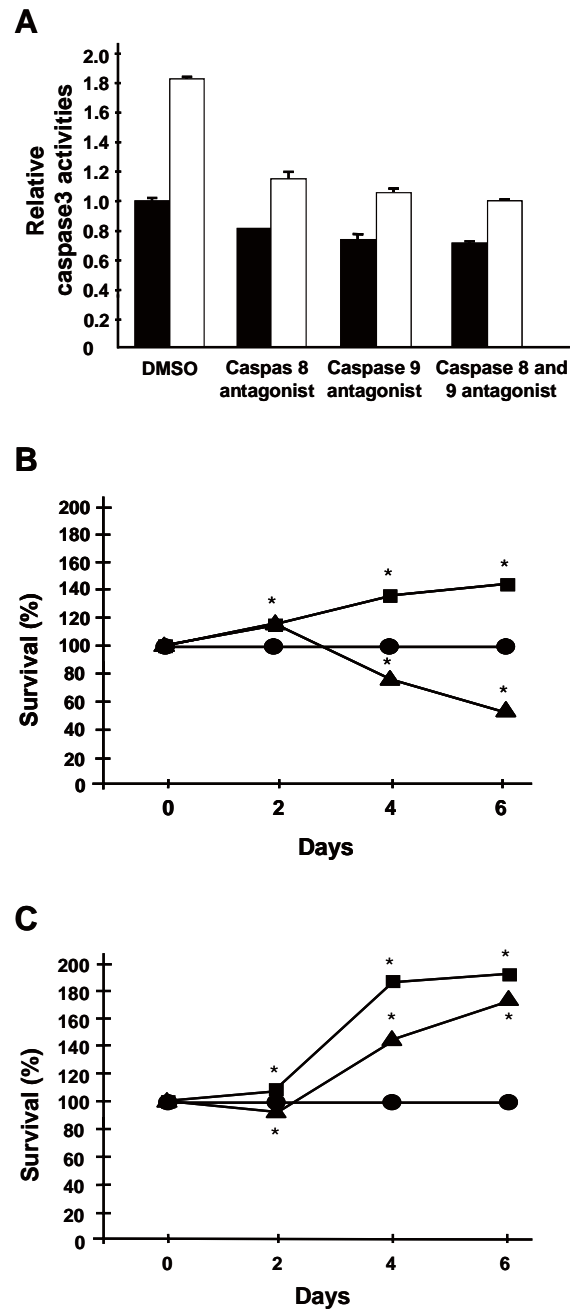


Figure 4. Variation of caspase 3 activity and survival rate by response to caspase 8 and 9 antagonists. A: Caspase 3 levels were measured in NIH3T3 cells cultured for 3 month (closed boxes) and SDHC E69 cells (open boxes) in the presence of caspase 8 and 9 antagonists. $n = 3$. B and C: Viability of NIH3T3 cells (B), SDHC E69 cells (C) grown in the presence of caspase 8 (■) and caspase 9 (▲) antagonists and DMSO (●) additions. $* p < 0.01$, $n = 3$.

cells (Figure 5D).

4. Discussion

We have previously established a transgenic SDHC E69 mouse cell line that contains a mutated SDHC subunit in complex II of the electron transport system (6). The SDHC E69 cells overproduced superoxide anion from mitochondria had elevated cytoplasmic carbonyl proteins and 8-OHdG in their DNA as well

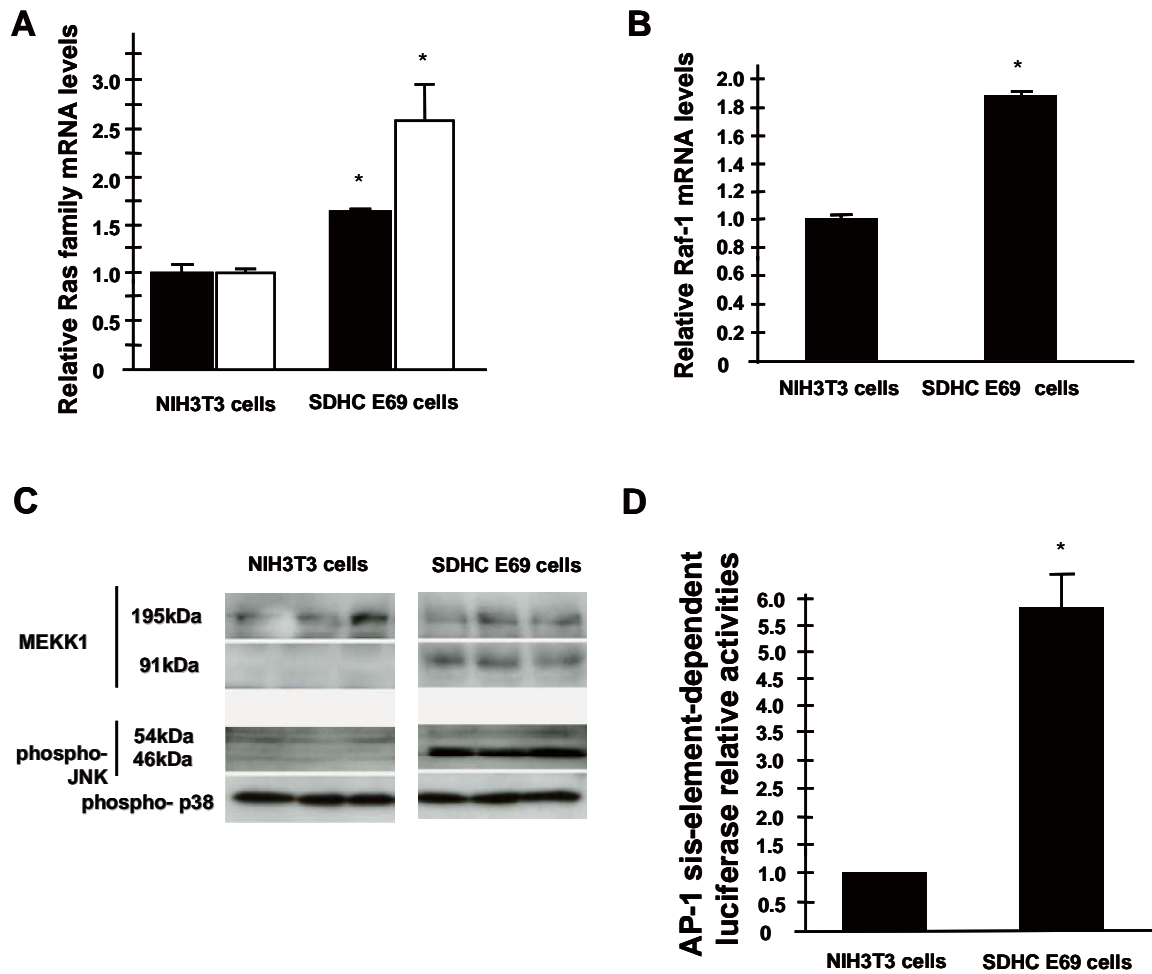


Figure 5. Alteration of stress-induced Ras-Raf and Ras-MEKK signal transduction pathways. A and B: Measurement of p21Ras (H-, N-, K-) (closed boxes), M-Ras (open boxes) (A) and Raf-1 mRNA expression levels (B) by Northern blot analysis. * $p < 0.01$, $n = 3$. C: Detection of MEKK1, phosphorylated JNK and p38 MAPK proteins, which are located and activated in downstream of MEKK1 activation, by Western blot analysis. $n = 3$. D: Measurement of transcriptional activation dependent on JNK activity by AP-1 cis-element-dependent luciferase activity. * $p < 0.01$, $n = 3$.

as significantly higher mutation frequencies than wild type (NIH3T3). There were many apoptotic cells in this cell line, as predicted by the observed increase in caspase 3 activity, decrease in mitochondrial membrane potential and structural changes in their mitochondria (6). In addition, some cells that escaped from apoptosis underwent transformation, as evidenced by the fact that SDHC E69 cells caused tumors within two weeks when injected under the epithelium of nude mice (Figure 1C) (6). The size of tumors remained unchanged even after one month (Figure 1D). It is known that NIH3T3 cells are transformed at high frequency by spontaneous mutations during long passage time or culture time. In fact, the cells, which did not proliferate within two weeks after the injection under the epithelium of nude mice, grew into huge malignant tumors one month (Figure 1A and B).

The SDHC E69-derived tumors showed no evidence of nuclear divisions and showed nuclear aggregation (Figure 2C). They had assumed the posture of a fibrous tumor, and the blood vessel and tumor border was not distinct. Moreover, tumor-associated cells were

present (Figure 2D). In contrast, as expected of actively proliferating neoplasms, the tumors derived from the NIH3T3 cells had evidence of the apocytes and the nuclear divisions with characteristic dense staining of the cytoplasm (Figure 2A). In addition, the margin between the tumor and the blood vessel was distinct (Figure 2B). Thus, the thickness of the tumor cells layer was less when derived from SDHC E69 cells versus the NIH3T3 cells (Figures 2E and F). These histological data are consistent with the notion that the NIH3T3 cells are actively proliferating while the SDHC E69 cells are not. We speculate that there was no increase in overall tumor mass because cell proliferation was counterbalanced by increased levels of apoptosis.

Mitochondria from SDHC E69 cells overproduced O_2^- , leading to wide-spread apoptosis as caspase 3 levels were elevated (6). Caspase 3 acts relatively late in the caspase cascade, after cells are inextricably committed to apoptosis. To elucidate the mechanisms by which overproduction of O_2^- leads to supernumerary apoptosis, we examined the activities of various components of the apoptotic machinery as well as the various signaling

pathways that promote apoptosis. We first examined cytosolic and mitochondrial levels of cytochrome c in the SDHC E69 cells after the establishment and their NIH3T3 progenitors. Cytochrome c is known to be released from mitochondria and combines with apoptosis protease activating factor-1 (Apaf-1), procaspase 9, and dATP in the cytosol, triggering the activation of caspase 3 (9). As expected given its role in electron transport, cellular cytochrome c was found in the mitochondria in both the SDHC E69 cells and NIH3T3 cells (Figure 3A). Cytosolic levels in the SDHC E69 cells and NIH3T3 cells were lower than mitochondrial levels. However, cytosolic cytochrome c levels increased significantly in the SDHC E69 cells. This is consistent with the increase in caspase 3 that we have documented previously (9) and suggests strongly that elevated O_2^- production in the SDHC E69 cells sets into motion events that enable cytochrome c leakage from mitochondria, with caspase 3 activation and apoptosis the downstream consequences. We then examined the status of two proapoptotic members of the Bcl-2 family. First, we looked at Bax, which regulates cytochrome c release from mitochondria by translocating from the cytoplasm to mitochondria and subsequently altering mitochondrial membrane permeability (10). Bax primarily localized to the cytosol. In the mitochondria of the SDHC E69 cells compared to NIH3T3 cells, the Bax levels were significantly higher (Figure 3A). These results suggest that the increased cytosolic cytochrome c levels observed in the SDHC E69 cells could be attributed at least in part to Bax translocation. Second, we analyzed the Bid protein, which is activated by caspase 8 cleavage to produce 15 kDa tBid. tBid translocates to mitochondria to facilitate cytochrome c release by interacting with Bax (11). Bid and tBid levels were barely detectable in the SDHC E69 cells (Figure 3A). These results suggest that cytochrome c release was mainly caused by Bax localized in mitochondria. We also examined the activation of the tumor suppressor gene p53, as p53 has long been known to act as a transcription factor to promote apoptosis via Bax action (12). More recently, p53 has been also been shown to localize to mitochondria and, in a transcription-independent fashion, play an important role in the mitochondrial apoptotic pathway (13). We asked whether p53 might be involved in the cellular responses to the oxidative stress inherent to the SDHC E69 cells. Since p53 levels are normally held low via the action of MDM2, we examined MDM2 mRNA expression using Northern blot analyses. MDM2 mRNA exists in three isoforms: 3.0 kbp, 1.7 kbp and several short-forms (of roughly 1.2 kbp) which are generated by alternative splicing. They are translated into several forms, including p90 (which possesses p53 binding capacity), p76 (which lacks p53 binding ability) and short-form types (which also lack p53 activity and are found in transformed cells) (14). In

NIH3T3 cells, MDM2 mRNA expression was equally distributed between the 3.0 kbp and 1.7 kbp mRNAs, which are translated into the p90 and p76 MDM2 proteins, respectively (Figure 3B). A dramatically different pattern was observed in the SDHC E69 cells, as only the short-form type was expressed, which is incapable binding to and promoting p53 protein degradation (Figure 3B). These results led us to test p53 protein levels by Western blot analysis. p53 levels were below the level of detection in NIH3T3 cells (Figure 3C). Conversely, p53 protein existed in copious amounts in the SDHC E69 cells, in which the short-form type MDM2 mRNA was expressed (Figure 3C). Moreover, most of the p53 protein was phosphorylated at serine residue 15 (Figure 3C), a modification known to activate p53 as a transcription factor, leading to cell-cycle arrest and apoptosis (15). These results strongly suggest that p53 exists as an active transcription factor in the SDHC E69 cells. We confirmed this in two ways. First, p21 protein, which is a p53 target gene and promotes the cell-cycle arrest, was highly expressed in the SDHC E69 cells but not in NIH3T3 cells (Figure 3C). Second, a luciferase-containing construct with a p53 binding cis-elements was transiently transfected into the each cell lines. Luciferase activity was over 2.8 times higher in the SDHC E69 cells than in the NIH3T3 cells (Figure 3D). Collectively, these data show that in the SDHC E69 cells, the oxidative stress resulting from mitochondrial overproduction of O_2^- leads to altered mRNA expression of MDM2 which in turn results in p53 accumulation and activation. As a consequence, p21 and presumably other p53 target genes are induced, resulting in cell-cycle delays and apoptosis. It is also possible that p53 is present in the mitochondria of the SDHC E69 cells to promote cytochrome c release and trigger apoptosis.

We next analyzed the relative roles played by caspase 8 and caspase 9 in elevated apoptosis in the SDHC E69 cells. Caspase 8 acts as an initiator caspase in the extrinsic apoptotic pathway while caspase 9 is activated by cytochrome c to initiate the intrinsic (mitochondrial) apoptotic pathway (9). When cleaved, both proteolytically activate executioner caspases such as caspase 3. We employed caspase 8 and 9 antagonists for this purpose and measured caspase 3 activity. As demonstrated previously, caspase 3 levels were higher in the SDHC E69 cells than in NIH3T3 cells (Figure 4A). In the NIH3T3 cells, caspase 3 activity was slightly decreased by each caspase antagonist ($p < 0.01$) (Figure 4A). Caspase 3 activity was not further reduced by addition of both caspase 8 and 9 antagonists in the NIH3T3 cells (Figure 4A). Since both caspase 8 and 9 participate in the extrinsic pathway, these results suggest that both caspases are active in NIH3T3 cells, albeit at low levels, in response to the low levels of extrinsic oxidative stress normally present in cultured cells. In the SDHC E69 cells, both

caspase 8 and caspase 9 inhibition had a larger effect on caspase 3 activity (Figure 4A). Since caspase 9 acts downstream of mitochondria, this suggests that the elevated apoptosis in the SDHC E69 transformed cells was the result of increased ROS generation in their mitochondria rather than involving the extrinsic pathway, in which case both caspase antagonists would be expected to have roughly equal inhibitory effects. Moreover, we tested the viability of cells cultured in the presence of each caspase antagonist. The survival rate of the NIH3T3 cells was decreased by treatment with a caspase 9 antagonist (Figure 4B). Some necrotic cell death was observed under these conditions (data not shown). Given that necrotic cell deaths were rarely observed in cells not treated with the caspase antagonists, we speculate that one consequence of the caspase 9-induced apoptosis is to protect tissues from stress-induced necrotic cell death that would otherwise result from mitochondrial oxidative stress.

In contrast to the results obtained with NIH3T3 cells, the presence of each caspase antagonist resulted in increased the cell growth and proliferation in the SDHC E69 cells (Figure 4C). This suggests that the SDHC E69 transformed cells might have developed oxidative stress resistance or even dependent cell growth and proliferation mechanisms. Moreover, both caspase 8 and 9 antagonists were inadequate to substantially reduce caspase 3 activity in the SDHC E69 cells ($p < 0.01$) (Figure 4A). This led us to speculate that a signal transduction pathway might be operative in these cells. Thus, while cytochrome c release from mitochondria was an important intermediary participant, components upstream of the mitochondria and independent of the mitochondria were responsible for initiating the apoptotic process in the SDHC E69 cells.

The Ras-Raf and Ras-MEKK signal transduction pathway has been shown to promote apoptosis in a mitochondria-independent fashion (16). For example, MEKK1 can be cleaved by many stimuli to generate a 91 kDa kinase that is a strong inducer of apoptosis (17,18). We tested to see if some of the elevated apoptosis in the 3-month SDHC E69 cells might be due to the activation of such signal transduction pathways. First, we analyzed p21Ras (H-, N-, K-Ras) and M-Ras mRNA expression levels by Northern blot analysis. Relative to the actin and G3PDH internal controls, p21Ras and M-Ras mRNA expression levels in the SDHC E69 cells were increased in comparison with the NIH3T3 cells (Figure 5A). Second, we tested Raf-1/C-Raf mRNA expression and MEKK1 protein concentration by Northern and Western blot analyses. Relative to the actin and G3PDH internal standards, Raf-1/C-Raf mRNA expression, which induces cell growth and proliferation, was significantly increased in the SDHC E69 cells in comparison to the NIH3T3 cells (Figure 5B). In addition, 195 kDa full-length MEKK1 protein, which can be cleaved to activate caspase 3,

was present in unchanged amount in the SDHC E69 cells, but the activated p91 kDa MEKK1 protein, which induces apoptosis independent of the mitochondrial pathway, was increased (Figure 5C). Thus, it appears that Ras acts to increase MEKK1 expression in response to the oxidative stress and MEKK1 has been cleaved into its active form in the SDHC E69 cells. In addition, we analyzed JNK and p38 MAPK, which are located further downstream in these signal transduction pathways. Activated 54 kDa and 46 kDa JNK proteins were present in increased amounts in the SDHC E69 cells (Figure 5C). Conversely, the accumulation of activated p38 MAPK protein was not altered (Figure 5C). We also performed an AP-1 cis-element-dependent luciferase assay, which serves as a measure of JNK activity. JNK-dependent transcription was activated in the SDHC E69 cells (Figure 5D).

We speculate that this explains the phenotypes we have previously observed in the SDHC E69 cells; namely, those of increased apoptosis, high levels of transformation into neoplasms and hypermutability. In addition, the growth characteristics of SDHC E69 cells in the epithelium of nude mice appear to mimic the slow growth of PGLs. It has been reported that the hereditary PGLs that are usually characterized by the development of benign, neural-crest-derived, slow-growing tumors of parasympathetic ganglia which are caused by mutations in the SDHC gene. Between 10% and 50% of cases are familial and are transmitted in an autosomal dominant fashion with incomplete and age-dependent penetrance. We speculate that these characteristics are related to the apoptosis induction caused by the mitochondrial.

Acknowledgements

We are indebted Ms. H. Mitani and Y. Hirayama, Cancer Institute, Japanese Foundation for Cancer Research, for the work using Nude mice. This work is supported by grant-in-aid for Scientific Research from the Ministry of Education, Culture, Sports, Science and Technology and for Aging Research from the Ministry of Health, Labor and Welfare, Japan and the Takeda Science Foundation.

References

1. Turrens JF. Superoxide production by the mitochondrial respiratory chain. *Biosci Rep* 1997; 17:3-8.
2. Ishii N, Fujii M, Hartman PS, Tsuda M, Yasuda K, Senoo-Matsuda N, Yanase S, Ayusawa D, Suzuki K. A mutation in succinate dehydrogenase cytochrome b causes oxidative stress and aging in nematodes. *Nature* 1998; 394:694-697.
3. Senoo-Matsuda N, Yasuda K, Tsuda M, Ohkubo T, Yoshimura S, Nakazawa H, Hartman PS, Ishii N. A defect in the cytochrome b large subunit in complex II causes both superoxide anion overproduction and

- abnormal energy metabolism in *Caenorhabditis elegans*. *J Biol Chem* 2001; 276:41553-41558.
4. Senoo-Matsuda N, Hartman PS, Akatsuka A, Yoshimura S, Ishii N. A complex II defect affects mitochondrial structure, leading to ced-3 and ced-4-dependent apoptosis and aging. *J Biol Chem* 2003; 278:22031-22036.
 5. Hartman PS, Ponder R, Lo HH, Ishii N. Mitochondrial oxidative stress can lead to nuclear mutability. *Mech Ageing Develop* 2004; 125:417-420.
 6. Ishii T, Yasuda K, Akatsuka A, Hino O, Hartman PS, Ishii N. A mutation in the SDHC gene of complex II increases oxidative stress, resulting in apoptosis and tumorigenesis. *Cancer Res* 2005; 65:203-209.
 7. Niemann S, Muller U. Mutations in SDHC cause autosomal dominant paraganglioma, type 3. *Nat Genet* 2000; 26:268-270.
 8. Baysal BE, Ferrell RE, Willett-Brozick JE, Lawrence EC, Myssiorek D, Bosch A, van der Mey A, Taschner PE, Rubinstein WS, Myers EN, Richard CW 3rd, Cornilisse CJ, Devilee P, Devlin B. Mutations in SDHD, a mitochondrial complex II Gene, in hereditary paraganglioma. *Science* 2000; 287:848-851.
 9. Budihardjo I, Oliver H, Lutter M, Luo X, Wang X. Biochemical pathways of caspase activation during apoptosis. *Annu Rev Cell Dev Biol* 1999; 15:269-290.
 10. Jürgensmeier JM, Xie Z, Deveraux Q, Ellerby L, Bredesen D, Reed JC. Bax directly induces release of cytochrome c from isolated mitochondria. *Proc Natl Acad Sci USA* 1998; 95:4997-5002.
 11. Luo X, Budihardjo I, Zou H, Slaughter C, Wang X. Bid, a Bcl2 interacting protein, mediates cytochrome c release from mitochondria in response to activation of cell surface death receptors. *Cell* 1998; 94:481-490.
 12. Shen Y, White E. p53-dependent apoptosis pathways. *Adv Cancer Res* 2001; 82:55-84.
 13. Mihara M, Erster S, Zaika A, Petrenko O, Chittenden T, Pancoska P, Moll UM. p53 has a direct apoptogenic role at the mitochondria. *Mol Cell* 2003; 11:577-590.
 14. Sigalas I, Calvert AH, Anderson JJ, Neal DE, Lunec J. Alternatively spliced mdm2 transcripts with loss of p53 binding domain sequences: transforming ability and frequent detection in human cancer. *Nat Med* 1996; 2:912-917.
 15. Shieh SY, Ikeda M, Taya Y, Prives C. DNA damage-induced phosphorylation of p53 alleviates inhibition by MDM2. *Cell* 1997; 91:325-334.
 16. Russell M, Lange-Carter CA, Johnson GL. Direct interaction between Ras and the kinase domain of mitogen-activated protein kinase kinase kinase (MEKK1). *J Biol Chem* 1995; 270:11757-11760.
 17. Widmann C, Gerwins P, Johnson NL, Jarpe MB, Johnson GL. MEK kinase 1, a substrate for DEVD-directed caspases, is involved in genotoxin-induced apoptosis. *Mol Cell Biol* 1998; 18:2416-2429.
 18. Gibson EM, Henson ES, Villanueva J, Gibson SB. MEK kinase 1 induces mitochondrial permeability transition leading to apoptosis independent of cytochrome C release. *J Biol Chem* 2002; 277:10573-10580.

(Received December 14, 2007; Revised January 22, 2008; Accepted January 25, 2008)